

Vortices and Defect Statistics in Two-Dimensional Optical Chaos

F. T. Arecchi,^(a) G. Giacomelli, P. L. Ramazza, and S. Residori

Istituto Nazionale di Ottica, Largo E. Fermi, 6, 50125 Firenze, Italy

(Received 1 April 1991)

We present the first direct experimental evidence of topological defects in nonlinear optics. For increasing Fresnel numbers F , the two-dimensional field is characterized by an increasing number of topological defects, from a single vortex, up to a large number of vortices with zero net topological charge. At variance with linear scattering from a fixed phase plate, here the defect pattern evolves in time according to the nonlinear dynamics. We assign the scaling exponents for the mean number of defects, their mean separation, and the charge unbalance as functions of F , as well as the correlation time of the defect pattern.

PACS numbers: 42.50.Tj, 05.45.+b

The role of defects in mediating turbulence in hydrodynamics systems with large aspect ratios has been investigated in fluid thermal convection [1], nematic liquid crystals [2], surface waves [3], analytic treatments [4(a)], and numerical simulations [4(b)] of partial differential equations in $2+1$ space-time dimensions. Their possible role in nonlinear optics has been discussed theoretically [5].

We present here the first experimental evidence of topological defects in nonlinear optics, and give their mean properties for increasing optical "aspect ratios," that is, for increasing Fresnel numbers. At variance with the material waves, which are easily visualized in terms of matter displacements, in the case of an optical field a phase measurement requires heterodyning against an external reference.

The experimental setup consists of a ring cavity where one-directional optical oscillations are generated by nonlinear interaction with a gain medium [a photorefractive $\text{Bi}_{12}\text{SiO}_{20}$ (BSO) crystal] pumped by a single-mode argon laser (Fig. 1). Control of the Fresnel number F is discussed in a previous report [6]. Reference [6] describes the dynamics of the optical field due to the nonlinear interaction among the transverse modes. The pro-

cess consists in the scattering of the pump field into the signal field confined in the ring cavity, via a refractive index grating generated in the BSO crystal by two-wave mixing. Because of an applied dc field across the BSO crystal, the grating drifts, yielding a detuning of a few hertz between pump and signal fields. Furthermore, diffusion and recombination processes provide a dissipative dynamics with a damping rate of the same order as the detuning frequency. This narrow bandwidth imposes a strong frequency pulling, and hence frequency degeneracy among the modes.

For small F the signal field is coherent in space even though fluctuating in time, namely, it is a single-mode regime where different transverse modes get excited one at a time in a regular sequence (periodic alternation) or in a chaotic sequence (chaotic itinerancy, as shown in numerical solutions of a complex Ginzburg-Landau equation [7]). For larger F , the field has a many-mode behavior, called STC (space-time chaos) whereby the local fluctuations display a non-Gaussian character, as expected from turbulence theories [8].

Phase information is extracted by beating the signal with a reference beam onto a charge-coupled-device (CCD) video camera. A topological defect of a complex field in two space dimensions is a singular point where the field amplitude goes to zero and its phase gradient has a circulation which is an integer number of 2π [9]. This integer is called the topological charge.

Figure 2(a) shows a single vortex at two different times. The dynamics is ruled by two different time scales, a short one T_s (around 1 sec) of the order of the damping time of the photorefractive medium [10] and a long one T_l (longer than 10 sec) corresponding to the jump from one mode to the other in the competition process (see Fig. 4 of Ref. [6]). In Fig. 2(a) the spiral arms rotate with a period T_s . The rotatory motion stops and then changes its sense of rotation on a time scale T_l . This amounts to saying that a charge of one sign leaves the domain and one of opposite sign enters. By a suitable algorithm [11] we reconstruct the instantaneous surfaces of phase as shown in Fig. 2(b) where the phase surface of a doughnut mode is a helix of pitch 2π around the defect.

When more than one vortex is present, in order to

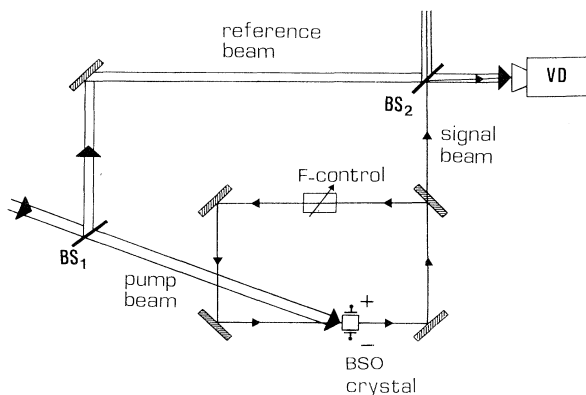


FIG. 1. Experimental setup. Details on the angular separation of pump and signal, on the pump intensity, on the cavity geometry, and on the F -control system were given in Ref. [6]. BS denotes beam splitter. VD is a CCD video camera.

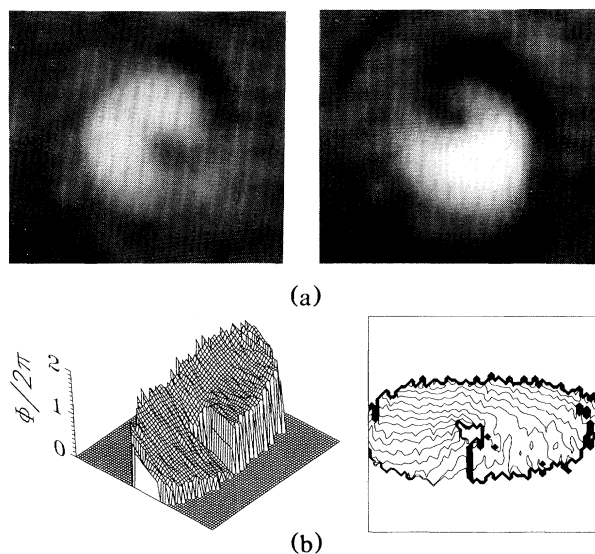


FIG. 2. (a) Single defect in a doughnut mode. Evidence of a vortex with a spiral wave around, which in the course of time changes its sense of rotation (left, clockwise; right, anticlockwise). (b) Reconstruction of the instantaneous phase surface for a vortex: perspective and equiphase plots.

resolve and count each vortex, we tilt the reference beam so that the video signal is now given by

$$I(x,y) = A^2 + B^2 + 2AB \cos[Kx + \Phi(x,y)],$$

where A and B are the amplitude of reference and signal fields, K is the fringe frequency due to tilting, x is the coordinate orthogonal to the fringes, and Φ is the local phase. This way, a phase singularity appears as a dislocation [12], and the topological charge is visually evaluated [13]. In the experiments reported in this Letter this charge is always ± 1 .

Figure 3(a) shows an intensity pattern as a doughnut with a phase singularity at the center. On a time scale T_1 , the doughnut splits into two separate intensity maxima with no phase singularity [Fig. 3(b)] and later the doughnut reappears but the singularity now has an opposite topological charge [Fig. 3(c)]. Notice that the rolls are a measuring tool and not an intrinsic characteristic of the system, as in hydrodynamic instabilities. Thus, they

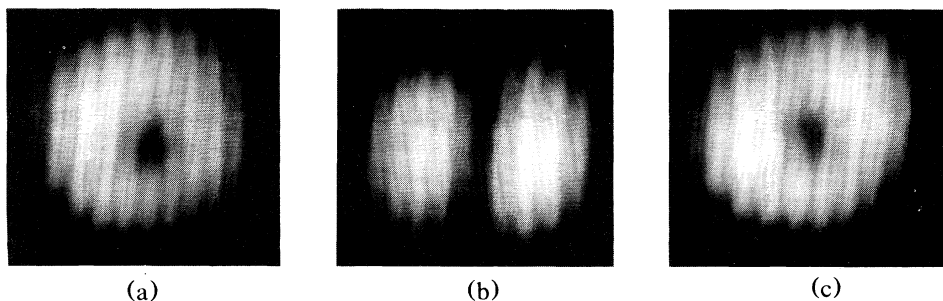


FIG. 3. Temporal sequence showing a mode switch with a vortex visualized as a dislocation via a tilted reference field. Inversion of topological charge from (a) to (c).

do not influence the defect number but only their resolution.

Topological defects in optics were originally observed by scattering through a random phase plate [12]. There are, however, profound differences which make the two phenomena qualitatively different. We list the main ones. (i) Our defects are closely linked to the ring oscillation. This is a threshold phenomenon which disappears for an applied dc field below 5 kV/cm. (ii) In the course of time, the nonlinear defect pattern evolves with the two characteristic times T_s and T_l mentioned above, whereas the defect pattern of a speckle field stands still, and it changes only by modification of the scattering medium (e.g., rotation of the phase plate). (iii) The linear defect pattern depends upon the random superposition of the scattered wavelets [14]; thus it changes shape if the detector position is moved with respect to the scatterer (Fig. 6 of Ref. [12]). On the contrary, in our experiment the defect pattern does not change for sizable detector displacements, and thus it depends only on the mode dynamics. This shows that the nonlinear field is truly two dimensional (defect lines parallel to the propagation direction), whereas the speckle field is not.

As we increase F , the dynamics of defects becomes more complex. We digitize the fringe system and count those defects separated by at least one fringe, in the region where fringes can be resolved. Figure 4(a) shows a configuration with an overall unbalance in the topological charge. A model of phase singularities in optics [15] displays regular patterns of defects with total nonzero charge. A heuristic explanation of Fig. 4(a) is that, for small F , the defect dynamics is strongly boundary dependent. Consequently we conjecture that an increase of F should eventually yield the thermodynamic limit of paired defects. This is indeed the case, as shown in Fig. 4(b), which refers to a high F and where the charge unbalance $U = |n_+ - n_-|$ (n_{\pm} denotes number of charges of the two signs) has become very small compared to the total number of defects, $N = n_+ + n_-$.

By averaging over a large number of frames for each F , we report in Figs. 5(a) and 5(b) the mean number $\langle N \rangle$ of defects per frame and the mean nearest-neighbor distance $\langle D_1 \rangle$ vs F . $\langle N \rangle$ and $\langle D_1 \rangle$ have a power-law dependence on F with exponents 1.79 ± 0.08 and -0.62 ± 0.04 . For

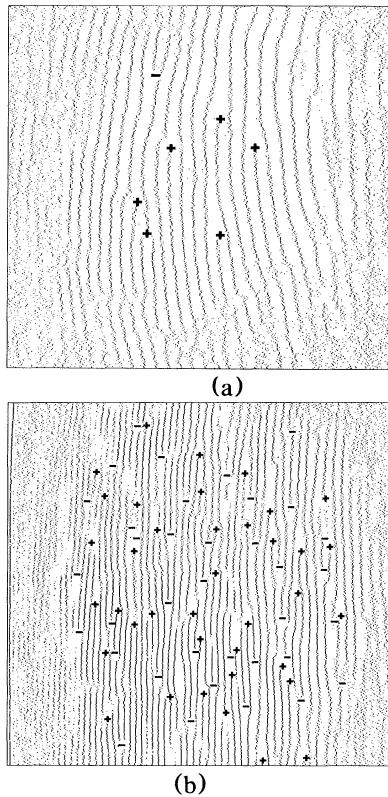


FIG. 4. Two examples of experimental configurations obtained by digitizing the fringe maxima. (a) $F \sim 3$: six defects of equal topological charge against one of opposite charge. (b) $F \sim 10$: about 70 defects of opposite charges, with a residual small charge unbalance.

convenience, we also plot the second- and third-neighbor separations $\langle D_2 \rangle$ and $\langle D_3 \rangle$.

Figure 5(c) gives the excess U normalized to the total defect number $N(U_n)$. For small apertures the dynamics is strongly boundary dependent and the excess is large. For increasing F , U_n decreases as a power law with exponent -1.20 ± 0.13 . Furthermore, measuring the space correlation functions of the intensity fluctuations, as done in Ref. [6], the corresponding correlation length ξ scales also as a power of F with an exponent -0.48 ± 0.05 [Fig. 5(d)].

The spatial disordering of defect positions is associated with the passage to STC. Viewing the dynamics of the optical field in the STC regime as ruled by a two-dimensional fluid of interacting defects [4], we expect that each defect occupies an area of diameter D . Since a phase singularity must be associated with a zero crossing of real and imaginary parts of the field, we conjecture that all intensity zeros are defects. But the diffractive treatment of optical cavities shows that the number N of intensity zeros for the highest allowed mode scales as the square of F ($N \sim F^2$) [16]. On the other hand, if a is the pupil aperture of the optical system, and D the average interdefect separation, we expect $N \sim a^2/D^2$, and, since

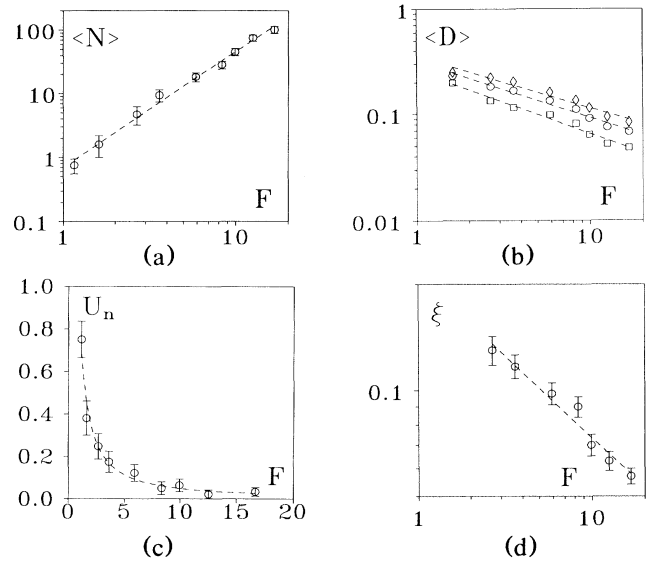


FIG. 5. (a) Mean number of defects $\langle N \rangle$ vs F . Best-fit exponent, 1.79 ± 0.08 . (b) Mean near-neighbor separations $\langle D_1 \rangle$ (squares), $\langle D_2 \rangle$ (circles), and $\langle D_3 \rangle$ (diamonds) vs F . Best-fit exponents, -0.62 ± 0.04 , -0.59 ± 0.03 , and -0.57 ± 0.03 . Here and in Fig. 6, all distances are normalized to the maximum size of the acquisition frame (512×512 points), and the error bars correspond to the data spread over many runs. (c) Normalized charge unbalance $U_n = |n_+ - n_-| / (n_+ + n_-)$ vs F . n_+ (n_-) is the total number of $+$ ($-$) defects. Best-fit exponent, -1.20 ± 0.13 . (d) Correlation length of the intensity fluctuations ξ vs F . Best-fit exponent, -0.48 ± 0.05 .

$a^2 \sim F$, then $D \sim F^{-0.5}$. Such scaling laws are approximately verified in Fig. 5; however, there are sizable deviations between heuristic and experimental exponents. A qualitative explanation of the first deviation is that $N \sim F^2$ holds only for the highest mode allowed by F , and instead our dynamics in the STC regime implies a strong configuration mixing. The $\xi \sim F^{-0.5}$ dependence of Fig. 5(d) shows that indeed STC is closely linked to the defect dynamics. Notice, from Figs. 5(b) and 5(d), that $\xi \sim \langle D_1 \rangle^{0.77}$, whereas the heuristic argument would provide $\xi \sim D$. This means that we cannot identify D with the nearest separation $\langle D_1 \rangle$, but we should somewhat average over $\langle D_1 \rangle$, $\langle D_2 \rangle$, etc. We can also justify the F dependence of U_n . Assume that unpaired defects are mainly created at the boundary, while in the bulk, pairs with compensated charge are created and destroyed. We conjecture that the total number N_c of boundary defects in the perimetral region of area aD scales as $N_c \sim aD/D^2 \sim a/\langle D_1 \rangle \sim F^{1.1}$, and the corresponding unbalance is $U \sim N_c^{1/2} \sim F^{0.55}$. Hence the normalized unbalance scales as $U_n \sim F^{0.55-1.8} = F^{-1.25}$, in good accord with the experiment. The heuristic consideration would instead provide $U_n \sim F^{-1.5}$.

F scalings of the defect numbers and of their mean sep-

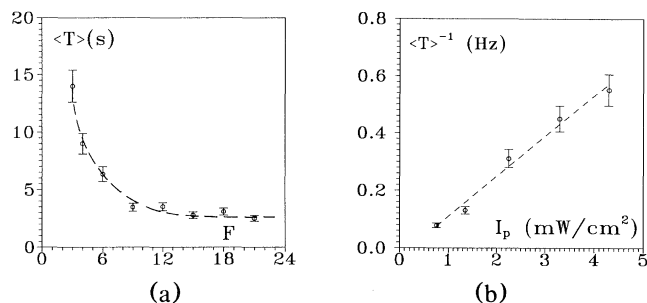


FIG. 6. (a) Mean separation time $\langle T \rangle$ between defect occurrence within a correlation domain vs the Fresnel number F , at a fixed pump intensity $P=2.25$ mW/cm². (b) Mean frequency of occurrence $1/\langle T \rangle$ vs P , at a fixed Fresnel number $F=8$.

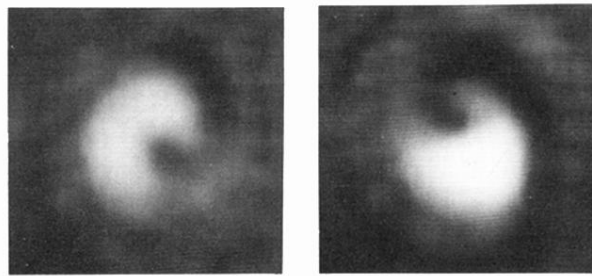
aration roughly equivalent to those reported in Fig. 5 are also found for linear defects [12]. The most crucial test of the nonlinear nature of the defects reported here is given by their time dependence. We select a small box of side ξ (a correlation domain) where generally there is zero or one defect present, and measure the occurrence time of events, where an event is the entrance of a defect into the box. This way, we build a sequence of time intervals, each defined by two successive events.

The corresponding mean separation $\langle T \rangle$ vs F is plotted in Fig. 6(a) for a fixed pump intensity P . Since for any setting of the control parameters F and P the time $\langle T \rangle$ is of the same order as the long-time scale T_l that characterizes the mode competition, we infer that mode jumping is mediated by the defect dynamics, as expected from the theory [4]. Figure 6(b) shows a linear dependence of $1/\langle T \rangle$ on the pump intensity. This effect, together with the threshold dependence on the dc field, is clear evidence of the nonlinear nature of the defects [17].

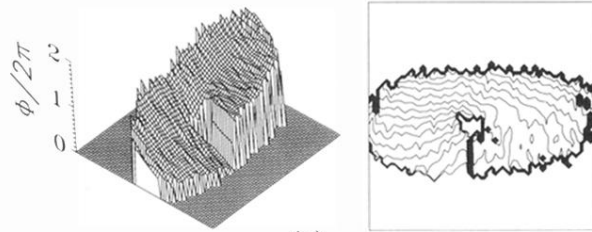
We are grateful to G. P. Puccioni for assistance in computation and to L. Gil and C. Perez Garcia for useful discussions. P.L.R. is holder of a CEO fellowship and S.R. of an Officine Galileo fellowship.

^(a)Also at Department of Physics, University of Firenze, Firenze, Italy.

- [1] G. Ahlers and R. P. Behringer, *Prog. Theor. Phys. Suppl.* **64**, 186 (1979); A. Pocheau, V. Croquette, and O. Le Gal, *Phys. Rev. Lett.* **55**, 1094 (1985).
- [2] R. Ribotta and A. Joets, in *Cellular Structures and Instabilities*, edited by J. E. Wesfried and S. Zaleski (Springer, Berlin, 1984); I. Rehberg, S. Rasenat, and V. Steinberg, *Phys. Rev. Lett.* **62**, 756 (1989); G. Goren, I. Procaccia, S. Rasenat, and V. Steinberg, *Phys. Rev. Lett.* **63**, 1237 (1989).
- [3] J. P. Gollub and R. Ramshankar, in *New Perspectives in Turbulence*, edited by S. Orszag and L. Sirovich (Springer, Berlin, 1990).
- [4] (a) K. Kawasaki, *Prog. Theor. Phys. Suppl.* **79**, 161 (1984); (b) P. Coullet, L. Gil, and F. Lega, *Phys. Rev. Lett.* **62**, 1619 (1989); E. Bodenschatz, W. Pesch, and L. Kramer, *Physica (Amsterdam)* **32D**, 135 (1988).
- [5] P. Coullet, L. Gil, and F. Rocca, *Opt. Commun.* **73**, 403 (1989).
- [6] F. T. Arecchi, G. Giacomelli, P. L. Ramazza, and S. Residori, *Phys. Rev. Lett.* **65**, 2531 (1990).
- [7] K. Otsuka, *Int. J. Mod. Phys. B* **5**, 1179 (1991).
- [8] P. C. Hohenberg and B. I. Shraiman, *Physica (Amsterdam)* **37D**, 109 (1989).
- [9] N. D. Mermin, *Rev. Mod. Phys.* **51**, 591 (1979).
- [10] J. L. Bougrenet de La Tocnaye, P. Pellat-Finet, and J. P. Huignard, *J. Opt. Soc. Am. B* **3**, 315 (1986).
- [11] M. Takeda, M. Ina, and S. Kobayashi, *J. Opt. Soc. Am.* **72**, 156 (1982).
- [12] N. B. Baranova, B. Ya. Zel'dovich, A. V. Mamaev, N. F. Pilipetskii, and V. V. Shkukov, *Zh. Eksp. Teor. Fiz.* **33**, 206 (1981) [*JETP Lett.* **33**, 195 (1981)].
- [13] D. Walgraef, *Structure Spatiales Loin de l'Equilibre* (Masson, Paris, 1988).
- [14] M. Berry, in *Physics of Defects*, edited by R. Balian *et al.* (North-Holland, Amsterdam, 1981), pp. 456–543.
- [15] M. Brambilla, F. Battipede, L. A. Lugiato, V. Penna, F. Prati, C. Tamm, and C. O. Weiss, *Phys. Rev. A* **43**, 5090 (1991).
- [16] See, e.g., A. E. Siegman, *Lasers* (University Sci. Books, San Francisco, 1987).
- [17] In Ref. [12] linear scattering was provided by a fixed phase plate. Early investigations on the time dependence of a linearly scattered field relied either on the artifact of a rotating scattering plate [F. T. Arecchi, E. Gatti, and A. Sona, *Phys. Lett.* **20A**, 27 (1966)] or on the Brownian motion of distributed scatterers [F. T. Arecchi, M. Giglio, and U. Tartari, *Phys. Rev.* **163**, 186 (1967)]. Anyway, time effects in linear scattering are *independent* of the pump intensity.

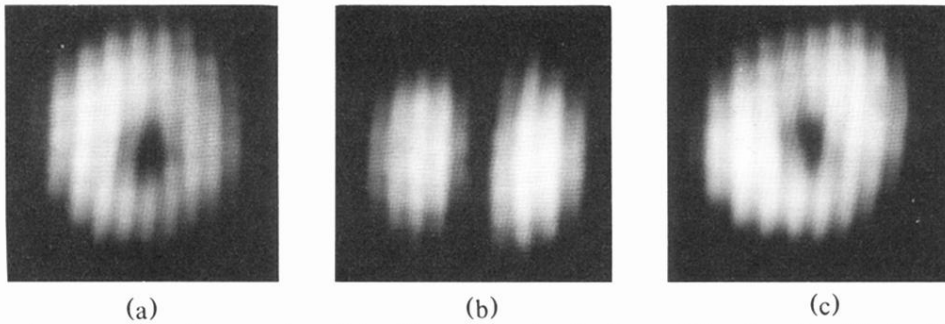


(a)



(b)

FIG. 2. (a) Single defect in a doughnut mode. Evidence of a vortex with a spiral wave around, which in the course of time changes its sense of rotation (left, clockwise; right, anticlockwise). (b) Reconstruction of the instantaneous phase surface for a vortex: perspective and equiphase plots.



(a) (b) (c)
FIG. 3. Temporal sequence showing a mode switch with a vortex visualized as a dislocation via a tilted reference field. Inversion of topological charge from (a) to (c).